

Diffusion models for Handwriting Generation

Troy Luhman*
troyluhman@gmail.com

Eric Luhman*
ericluhman2@gmail.com

Abstract

In this paper, we propose a diffusion probabilistic model for handwriting generation. Diffusion models are a class of generative models where samples start from Gaussian noise and are gradually denoised to produce output. Our method of handwriting generation does not require using any text-recognition based, writer-style based, or adversarial loss functions, nor does it require training of auxiliary networks. Our model is able to incorporate writer stylistic features directly from image data, eliminating the need for user interaction during sampling. Experiments reveal that our model is able to generate realistic, high quality images of handwritten text in a similar style to a given writer. Our implementation can be found at <https://github.com/tcl9876/Diffusion-Handwriting-Generation>.

1 Introduction

Deep generative models have been able to produce realistic handwritten text. Handwriting data can be stored in online or offline format. Online data is rendered as a sequence of pen strokes, and offline data is stored directly as an image. Online temporal data is easier to work with due to its lower dimensionality, but is harder to collect since each stroke must be recorded during writing. Each sample of handwriting data is associated with a text sequence label describing the content of the handwritten text. Each handwritten sample can also be associated with another example of handwriting from the same writer, which provides information about the style of the writer.

The task of handwriting generation was first done by (Graves, 2013), who used a RNN to synthesize online handwriting. Since then, most work on online handwriting generation has used an RNN based architecture, while most work on offline handwriting generation has used a GAN. Both methods have been able to generate realistic, diverse samples in a given writer's handwriting style. RNN based models (Chung et al., 2015; Aksan et al., 2018; Kotani et al., 2020) are simple to train and sample from, but one challenge they face is that they require the writer style data to be in online format. This poses a challenge for incorporating stylistic information, as the user's pen strokes must be recorded during sampling. GAN based methods for handwriting generation (Alonso et al., 2019; Kang et al., 2020; Fogel et al., 2020) have been used as an alternative to online autoregressive models. GAN based methods have the advantage of being able to incorporate offline stylistic information, as they work with images directly. The downside to GAN-based methods is that they can be difficult to train and may suffer from lack of diversity due to mode collapse. Additionally, previous work on GAN-based handwriting generation requires training at least two auxiliary networks: the discriminator and a text recognition network to control the content of the generated text.

Diffusion probabilistic models (Sohl-Dickstein et al., 2015; Ho et al., 2020) use a Markov chain to convert a known distribution (e.g. Gaussian) into a more complex data distribution. A diffusion process converts the data distribution into a simple distribution by iteratively adding Gaussian noise to the data, and the generative model learns to reverse this diffusion process. Diffusion models can be trained to optimize a weighted variational lower bound of the data likelihood. This objective is similar to that

*Equal contribution

of noise conditional score networks (Song and Ermon, 2019), which estimates the gradients of the data distribution. Both noise conditional score networks and diffusion models generate samples by starting from Gaussian noise and gradually removing this noise.

In this paper, we propose a diffusion probabilistic model for online handwriting generation. Our proposed model has advantages over both autoregressive and GAN based methods of handwriting generation. Our model, though it generates samples in online format, is able to incorporate writer stylistic features from offline data, eliminating the need for user interaction during sampling. Our method of handwriting generation does not require using any text based, style based, or adversarial loss functions, nor does it require training of auxiliary networks. As a result, our model has a very simple training and sampling procedure. Our model is able to generate realistic samples of handwritten text in a similar style to the original writer.

2 Diffusion Models for Handwriting Generation

2.1 Diffusion Probabilistic Models

Let $q(y_0)$ be the data distribution, and let y_1, \dots, y_T be a series of T latent variables with the same dimensionality as y_0 . A diffusion model consists of two processes: a noise adding diffusion process, and a reverse process (Sohl-Dickstein et al., 2015). The posterior $q(y_{1:T} | y_0)$, or the diffusion process, is defined as a fixed Markov chain where Gaussian noise is added at each iteration based on a fixed noise schedule β_1, \dots, β_T :

$$q(y_{1:T} | y_0) = \prod_{t=1}^T q(y_t | y_{t-1}), \quad q(y_t | y_{t-1}) = \mathcal{N}(y_t; \sqrt{1 - \beta_t}y_{t-1}, \beta_t \mathbf{I}) \quad (1)$$

The reverse process is defined as a Markov chain parameterized by θ :

$$p(y_T) = \mathcal{N}(y_T; 0, \mathbf{I}), \quad p_\theta(y_{0:T}) = p(y_T) \prod_{t=1}^T p_\theta(y_t | y_{t-1}) \quad (2)$$

where $p_\theta(y_{t-1} | y_t)$ intends to reverse the effect of the noise adding process $q(y_t | y_{t-1})$:

$$p_\theta(y_{t-1} | y_t) = \mathcal{N}(y_{t-1}; \mu_\theta(y_t, t), \Sigma_\theta(y_t, t)) \quad (3)$$

where $\Sigma_\theta(y_t, t) = \sigma_t^2 \mathbf{I}$ and σ_t^2 is a constant related to β_t . The forward process posterior is defined as:

$$q(y_{t-1} | y_t, y_0) = \mathcal{N}(y_{t-1}; \tilde{\mu}(y_t, y_0), \sigma_t^2 \mathbf{I}) \quad (4)$$

(Ho et al., 2020) showed that the ELBO can be calculated in closed form by expanding it into a series of KL Divergences between Gaussian distributions:

$$\mathbf{ELBO} = -\mathbb{E}_q \left(D_{KL}(q(y_T | y_0) \| p(y_T)) + \sum_{t=2}^T D_{KL}(q(y_{t-1} | y_t, y_0) \| p_\theta(y_{t-1} | y_t)) - \log p_\theta(y_0 | y_1) \right) \quad (5)$$

By defining some constants, y_t can be calculated in closed form for any step t :

$$\alpha_t = 1 - \beta_t, \quad \bar{\alpha}_t = \prod_{s=1}^t \alpha_s, \quad \epsilon \sim \mathcal{N}(0, \mathbf{I}), \quad y_t = \sqrt{\bar{\alpha}_t}y_0 + \sqrt{1 - \bar{\alpha}_t}\epsilon \quad (6)$$

The loss function then becomes the following for some timestep $t - 1$, where μ_θ is a model that predicts the forward process posterior mean $\tilde{\mu}$:

$$L_{t-1} = E_{y_0, \epsilon} \left(\left\| \frac{1}{2\sigma^2} \left\| \frac{1}{\sqrt{\alpha_t}} \left(y_t - \frac{\beta_t}{\sqrt{1 - \bar{\alpha}_t}} \epsilon \right) - \mu_\theta(y_t, t) \right\|^2 \right) \right) \quad (7)$$

(Ho et al., 2020) observed that diffusion probabilistic models can be reparameterized to resemble score-based generative models (Song and Ermon, 2019). Score-based generative models estimate the gradient of the logarithmic data density $\nabla_x \log(p(x))$ with a denoising objective. Under this reparameterization, the diffusion model, ϵ_θ , predicts ϵ similar to the objective of score-based models. The loss function for predicting ϵ becomes:

$$L_{t-1} = \mathbb{E}_{t,\epsilon} [C_t \|\epsilon - \epsilon_\theta(y_t, t)\|_2^2], C_t = \frac{\beta^2}{2\sigma_t^2 \alpha_t (1 - \bar{\alpha}_t)} \quad (8)$$

During sampling, diffusion probabilistic models iteratively remove the noise added in the diffusion process, by sampling y_{t-1} for $t = T, \dots, 1$:

$$y_{t-1} = \frac{1}{\sqrt{a_t}} \left(y_t - \frac{\beta_t}{\sqrt{1 - \bar{\alpha}_t}} \epsilon_\theta(y_t, t) \right) + \sigma_t z \quad (9)$$

where $z \sim \mathcal{N}(0, \mathbf{I})$ and σ_t is a constant related to β_t . For our experiments, we used $\sigma_t^2 = \beta_t$.

In our experiments, we found it beneficial to make a modification to the original sampling procedure. First, as our model predicts ϵ , we can use the estimate of ϵ to approximate y_0 at any timestep t :

$$y_0 \approx \hat{y}_0 = \frac{1}{\sqrt{\bar{\alpha}_t}} (y_t - \sqrt{1 - \bar{\alpha}_t} \epsilon_\theta(y_t, t)) \quad (10)$$

We now use our approximation for y_0 to find y_{t-1} :

$$y_{t-1} = \sqrt{\bar{\alpha}_{t-1}} \hat{y}_0 + \sqrt{1 - \bar{\alpha}_{t-1}} z, z \sim \mathcal{N}(0, \mathbf{I}) \quad (11)$$

We first estimate \hat{y}_0 from y_t and ϵ_θ using Equation 10, then find y_{t-1} according to Equation 11. Combining these two, we get:

$$y_{t-1} = \frac{1}{\sqrt{\bar{\alpha}_t}} (y_t - \sqrt{1 - \bar{\alpha}_t} \epsilon_\theta(y_t, t)) + \sqrt{1 - \bar{\alpha}_{t-1}} z, z \sim \mathcal{N}(0, \mathbf{I}) \quad (12)$$

The training procedure is performed by minimizing Equation 8 with the C_t term removed. We compared sampling y_{t-1} according to Equation 12 as opposed to Equation 9 and found that the Equation 12 led to more realistic samples (see ablation study in Table 1), at the cost of a slight decrease in diversity.

2.2 Conditional Handwriting Generation

they were alone together.

a small qn outbuilding

He said these concerned Mr. Weaver's
was quick to see how much
a definite disadvantage.

begin! Why tell them you are a novice

Figure 1: Samples from the IAM Database.

We will now address the task of conditional online handwriting generation. Each data point x_0 is composed of a sequence of N vectors $x_1 \dots x_N$. Each individual vector in the sequence $x_n \in \mathbb{R}^2 \times \{0, 1\}$ is composed of a real valued pair which represents the pen offset from the previous stroke in the x and y direction, and a binary entry that has a value of 0 if the pen was down when writing the stroke and 1 otherwise. Each handwritten sequence is associated with a discrete character sequence c describing what was written. Each sequence is also associated with an offline image containing writer’s style information, denoted by s .

There is one technical issue that needs to be addressed. The reverse process in Equation 3 is parameterized by a Gaussian distribution. We cannot parameterize the binary variable representing whether the stroke was drawn by a Gaussian distribution as we did for the real valued pen strokes. However, we can instead parameterize it with a Bernoulli distribution, which can also be optimized in closed form.

We therefore split each data point x_0 into two sequences y_0 and d_0 of equal length, with y_0 representing the real valued pen strokes, and d_0 representing whether the stroke was drawn. At each step t , our model $d_\theta(y_t, c, s, \sqrt{\bar{\alpha}})$ returns an estimate \hat{d}_0 of whether the pen was down. d_θ shares all parameters with ϵ_θ . Our stroke loss and pen-draw loss are shown in Equations 13 and 14:

$$L_{\text{stroke}}(\theta) = \|\epsilon - \epsilon_\theta(y_t, c, s, \sqrt{\bar{\alpha}})\|_2^2 \tag{13}$$

$$L_{\text{drawn}}(\theta) = -d_0 \log(\hat{d}_0) - (1 - d_0) \log(1 - \hat{d}_0) \tag{14}$$

We found it beneficial to weight the pen-draw loss according to the noise level, since it is more difficult to predict the pen-draws at higher noise levels. We weight Equation 14 by $\bar{\alpha}$ during training (see Algorithm 1).

(Song and Ermon, 2019, 2020) noted that the choice of noise schedule is crucial to generating high quality samples. (Chen et al., 2020) proposed to condition the model on the continuous noise level $\sqrt{\bar{\alpha}}$ as opposed to the discrete index t . This allows for the use of different noise schedules during sampling without retraining the model. In order to condition the network on the continuous noise level, we first define noise schedule l where $l_0 = 1, l_t = \sqrt{\bar{\alpha}_t}$. During training, we condition the model on $\sqrt{\bar{\alpha}} \sim \text{Uniform}(l_{t-1}, l_t)$, where $t \sim \text{Uniform}(\{1, \dots, T\})$.

One desirable property of handwriting synthesis networks is the ability to generate handwriting in the style of a given writer. Previous handwriting synthesis methods are able to control the style of the generated handwriting by conditioning on a sample written by the writer. Although our model generates online output samples, our model accepts offline images as input for writer stylistic features. Previous RNN-based models require online data during sampling, which is difficult to collect. To incorporate style information, we extract features from the image using Mobilenet (Sandler et al., 2018) and use these features as input to our model.

We describe our training procedure in Algorithm 1 and our sampling procedure in Algorithm 2. Note that our training procedure does not require training any auxiliary networks and does not use text recognition or style-based losses.

Algorithm 1: Training	Algorithm 2: Sampling
<pre> 1 while not converged do 2 $y_0 \sim q(y_0)$ 3 $t \sim \text{Uniform}(\{1, \dots, T\})$ 4 $\sqrt{\bar{\alpha}} \sim \text{Uniform}(l_{t-1}, l_t)$ 5 $\epsilon \sim \mathcal{N}(0, \mathbf{I})$ 6 $y_t = \sqrt{\bar{\alpha}}y_0 + \sqrt{1 - \bar{\alpha}}\epsilon$ 7 Take gradient descent step on: 8 $\nabla_{\theta}(L_{\text{stroke}}(\theta) + \bar{\alpha}L_{\text{drawn}}(\theta))$ 9 end </pre>	<pre> 1 $y_T \sim \mathcal{N}(0, \mathbf{I})$ 2 for $t = T, \dots, 1$ do 3 $z \sim \mathcal{N}(0, \mathbf{I})$ 4 $y_{t-1} = \frac{1}{\sqrt{\bar{\alpha}_t}}(y_t - \sqrt{1 - \bar{\alpha}_t}\epsilon_{\theta}(y_t, c, s, \sqrt{\bar{\alpha}_t}))$ 5 $y_{t-1} = y_{t-1} + \sqrt{1 - \bar{\alpha}_{t-1}}z$ if $t > 1$ 6 $d_0 = d_{\theta}(y_t, c, s, \sqrt{\bar{\alpha}_t})$ 7 end 8 return y_0, d_0 </pre>

3 Model Architecture

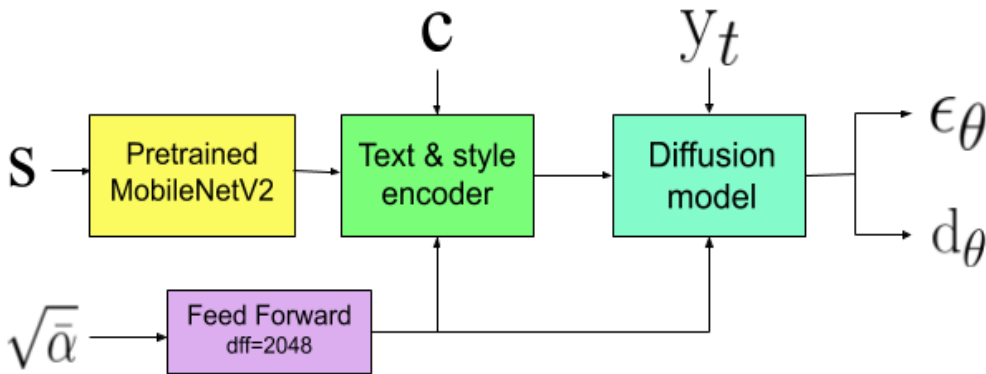


Figure 2: Overview of our full model.

Our full model is shown in Figure 2. It consists of two parts: a text and style encoder to represent the desired text and stylistic features, and a diffusion probabilistic model to predict ϵ_{θ} . The noise level $\sqrt{\bar{\alpha}}$ is passed through a feedforward network consisting of two fully connected layers. Both the encoder and the diffusion model are conditioned on the noise level.

Conditioning on the noise level: To condition our model on the noise level, we use affine transformations along the channel axis. Each affine transformation’s scales and biases are parameterized by the output of a fully connected layer. Our affine transformation is detailed in Figure 6 in Appendix A.

Text and Style Conditioning: For writer conditioning, we first extract local features from an image of their handwriting using a MobileNetV2 (Sandler et al., 2018) pretrained on Imagenet. Character-level embeddings are used to represent the text sequence. We then compute attention between the text sequence and the extracted features, allowing different text characters to attend to different portions of the given writer sample. This output is then added to the text sequence representation, before being passed through a feedforward network. Full architectural details on the encoder can be seen in Figure 10 in Appendix A.

Diffusion model: Our diffusion model consists of downsampling blocks, followed by upsampling blocks, and uses long range convolutional skip connections. We use two main types of blocks, convolutional blocks and attentional blocks. Full information on our diffusion model architecture is detailed in Figure 9 in Appendix A.

Our convolutional blocks consist of 3 convolutional layers and a convolutional skip connection. We apply conditional affine transformations to the output of every convolutional layer. Further architectural information on our convolutional block is shown in Figure 7 in Appendix A.

Our attentional blocks consist of 2 multi-head attention layers, and a feed forward network. The first attention layer performs attention between the stroke sequences x and the output of the text-style encoder, while the second performs self-attention. Sinusoidal positional encodings (Vaswani et al., 2017) are added to the queries and keys at every attentional layer. For attentional layers at higher stroke resolutions, the positions of the text sequence are multiplied before the positional encoding to allow for easier alignment between the text sequence and the longer stroke sequence. We use layer normalization (Ba et al., 2016) followed by conditional affine transformations after every attentional layer and feed forward network. Further architectural information on our attentional block is shown in Figure 8 in appendix A.

4 Related Work

Our work builds off previous work on diffusion probabilistic models (Sohl-Dickstein et al., 2015; Ho et al., 2020) and Noise Conditional Score Networks or NSCNs (Vincent, 2011; Song and Ermon, 2019), which are closely related. (Ho et al., 2020) addressed the task of image generation using a diffusion model, and (Kong et al., 2020; Chen et al., 2020) used diffusion models for speech generation. (Song and Ermon, 2019, 2020) used NSCNs for image generation, and (Cai et al., 2020) used NSCNs for shape generation. (Jolicoeur-Martineau et al., 2020) combined the NCSN objective with an adversarial objective to address image generation.

Handwriting synthesis was first explored in (Graves, 2013), which used a recurrent neural network (RNN) to predict each stroke one at a time. Since then, most work on online handwriting generation has made use of a type of RNN known as a Variational RNN (Chung et al., 2015). Variational RNNs (VRNNs) incorporate a Variational Autoencoder (Kingma and Welling, 2014), or VAE, at each timestep to generate sequences. (Aksan et al., 2018) uses a conditional VRNN that is able to separate content and style elements, allowing for editing of the generated samples. (Kotani et al., 2020) incorporates character and writer level style information for further model flexibility. RNN based architectures exhibit high quality, diverse samples and have many capabilities. These drawbacks of autoregressive models is that they accept online writing examples in order to incorporate the writer’s stylistic information, requiring the writer to interact during sampling. (Mayr et al., 2020) alleviates this problem by approximating an online representation of an offline image with the downside being that it is highly dependent on the performance of the approximation model.

As an alternative to autoregressive RNN models, generative adversarial networks (GANs) (Goodfellow et al., 2014) have been proposed for handwriting synthesis. (Alonso et al., 2019) first used a GAN to generate images of handwritten words. (Kang et al., 2020; Fogel et al., 2020) both use the GAN framework and improve sample quality over (Alonso et al., 2019), in addition to being able to condition on writer stylistic features. GAN based methods of handwriting generation are not autoregressive, and are able to condition on offline style features, which is beneficial since no user interaction is required during sampling. The downside of GANs is that adversarial training procedure of GANs can be unstable and result in mode collapse, which reduces the diversity of samples produced. Previous works on handwritten text generation with GANs also have used a text recognition objective for the generated samples which can complicate the training procedure.

5 Experiments

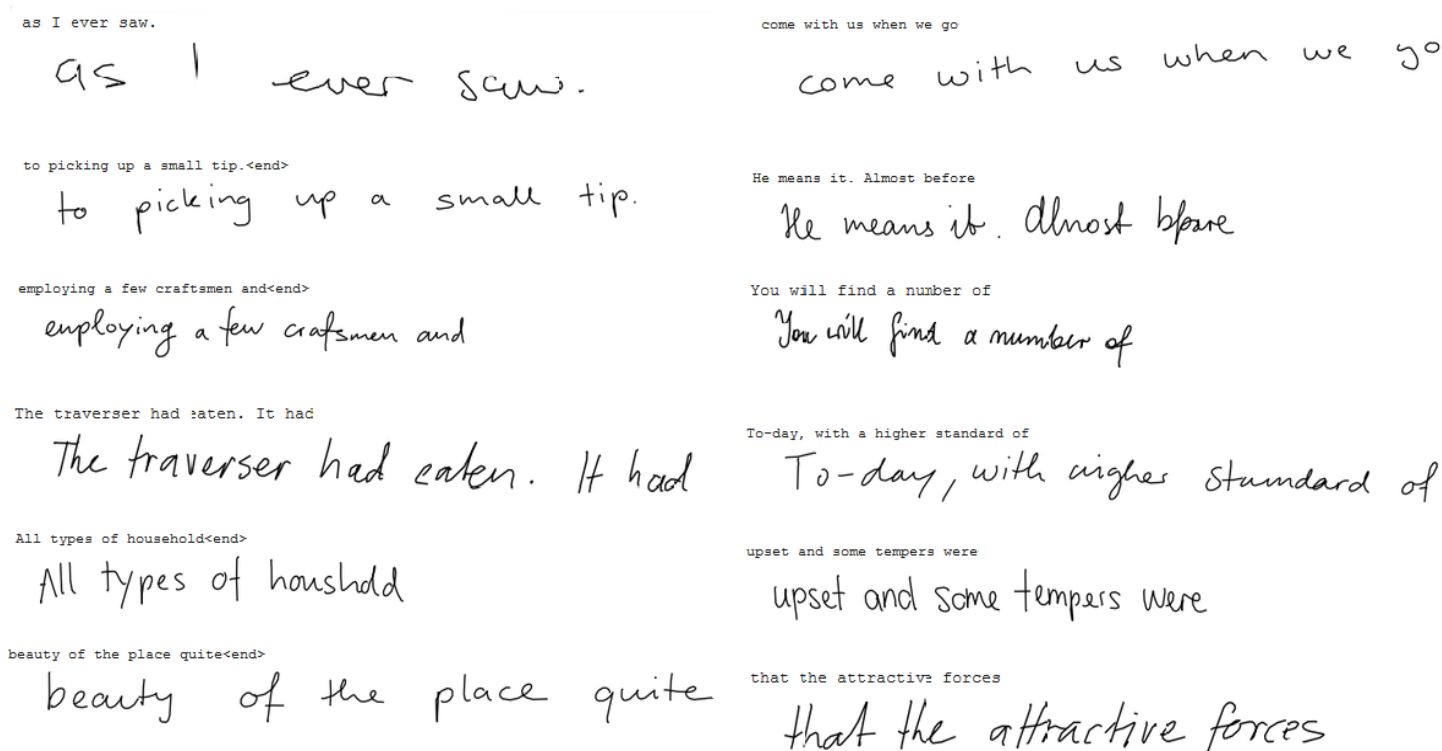


Figure 3: Four of the above samples are real, drawn from the test dataset. The remaining 8 were randomly generated by our model. We encourage the reader to try to determine which ones are fake, and which are real. Answer in Appendix B

5.1 Experiment Details

We use the IAM Online Database (Liwicki and Bunke, 2005), a dataset of approximately 12000 handwritten lines that are each associated with a character string label. Each sample is also associated with an sample of handwritten text by the writer, which we store as an offline image. We use the same splits as (Graves, 2013). To preprocess the data, we first divide each example by its standard deviation. We discard samples containing strokes of lengths 15 standard deviations above the mean. These very long strokes usually are a result of large spacing between words. We combine strokes pointing in approximately the same direction as their neighbor, which reduces the dimensionality without visual differences.

We used $T = 60$ diffusion steps for our models. For our choice of noise schedule β_1, \dots, β_T , we used $\beta_t = 0.02 + \text{Exponential}(1 \times 10^{-5}, 0.4)$. $\text{Exponential}(1 \times 10^{-5}, 0.4)$ denotes a geometric sequence from 1×10^{-5} to 0.4. We trained our model for 60000 steps with a batch size of 96 on a single Nvidia V-100. We use the Adam optimizer (Kingma and Ba, 2017) with $\beta_1 = 0.9$, $\beta_2 = 0.98$, and we clip the norm of the gradients to 100. For our learning rate, we use the inverse square root schedule in (Vaswani et al., 2017) with 10000 warmup steps and the d_{model} argument at 256. All our models have the same size of 10.0 million parameters. These values were not swept over.

We evaluate the performance of our models with Frechet Inception Distance (FID) (Heusel et al., 2017) and Geometry Score (GS) (Khruikov and Oseledets, 2018). FID uses the InceptionV3 network (Szegedy et al., 2016) to compare the similarity of real images to generated images. Since our model outputs online sequences as output, we first plot the sequences and then convert them to offline images. The Geometry score compares the geometric properties of the real and generated data manifolds to measure quality and diversity.

To conduct the experiment, we draw two sets of 4500 examples from the training dataset. We compare the first set of examples with our model’s predictions of the second set of examples given the corresponding text and style information. For the FID evaluation, we resize all the plotted images to size $M \times N$. For the Geometry Score evaluation, we keep the generated data in online form, and use the same values of L_0, γ, i_{max} as (Khrulkov and Oseledets, 2018). We run both experiments once.

5.2 Results and Discussion

We report our scores for the objective evaluation metrics in Table 1.

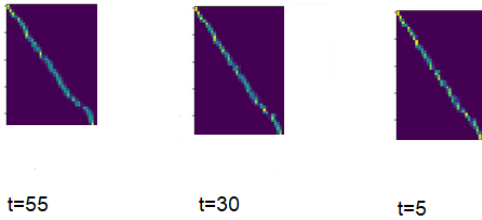
Table 1: Objective evaluation metrics (lower is better)

	FID	GS
Ground Truth	2.91	5.4×10^{-4}
Our Model	7.10	3.3×10^{-3}
Ablated Model	8.05	2.7×10^{-3}

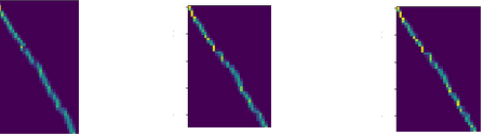
Due to differences in the dataset and format of the generated output, we do not directly compare our results with previous works. Our images for FID are first plotted on a graph, then the graph is converted to an image. This is in contrast to previous methods that used FID, which generated offline images directly. Our GS is computed from online data, which cannot be compared with scores from offline data. We instead compare our results with online samples from the dataset itself. The ground truth score is calculated with the real examples in the second set as opposed to the model’s predictions of examples in the second set.

Ablation Study We conduct an ablation study to compare the quality of samples generated with our sampling procedure (in Algorithm 2) to those generated with the original sampling procedure, which uses Equation 9. We compare FID and GS for the generated samples in Table 1. We used the same trained model for both models, and only changed the sampling procedure. We found that in the case of online handwriting generation, our sampling procedure yielded relatively higher FID scores but relatively lower Geometry Score. For qualitative comparison between the two, see Figures 15 and 16 in the Appendix.

Attention Weights Learning to properly align the text sequence to the stroke sequence is critical for generating longer sequences of realistic text without missing, misplaced or confused letters. The diagonal line in Figure 4 represents the predicted alignment between the strokes and the text sequence. Empirically, when the attention weights diverged from the diagonal line, this led to spelling mistakes. We observed that the text-to-stroke attention weights remain well-aligned throughout the reverse process, even in the earliest stages where the text itself is not recognizable.



The traverser had eaten the lead



administrative complication

Figure 4: Text - to - stroke attention weights at $t = 5, t = 30, t = 55$. The diagonal line shows the alignment predicted by the model between the strokes and the texts.

Style Interpolation Given two samples of handwriting from two different writers, we would like to be able to interpolate a sample that shares stylistic aspects with both writers. In order to incorporate style information, our model accepts a feature vector s that is obtained by extract features from the given image using MobileNet. To perform style interpolation, we first obtain feature vectors s'_0, s'_1 from s_0, s_1 and condition our model on \hat{s} , where $\hat{s} = \lambda s'_0 + (1 - \lambda)s'_1$. $\lambda \in [0, 1]$ controls the relative importance of s'_0 .



Figure 5: Style Interpolation. The top and bottom images s_0, s_1 contain writer style information and are drawn from the test dataset. To perform style interpolation, we keep the generated text constant, and gradually decrease λ . The generated samples share calligraphic aspects with the bottom picture s_1 more and less with the top picture s_0 less as λ decreases.

6 Conclusion

In this paper, we have proposed a diffusion probabilistic model for online handwriting generation. Our work builds off of previous work in both diffusion probabilistic models (Ho et al., 2020), and closely related score based generative models (Song and Ermon, 2019). Our training procedure is more simple than most previous handwriting generation methods, as ours does not require adversarial, text-recognition based or writer-recognition based objectives. We also demonstrate the ability for our model to incorporate calligraphic features from offline data, which is easier to collect during sampling time. Empirically, the samples from our model are realistic and diverse.

References

- E. Aksan, F. Pece, and O. Hilliges. Deepwriting: Making digital ink editable via deep generative modeling, 2018.
- E. Alonso, B. Moysset, and R. Messina. Adversarial generation of handwritten text images conditioned on sequences, 2019.
- J. Ba, J. Kiros, and G. Hinton. Layer normalization. 07 2016.
- A. Block, Y. Mroueh, A. Rakhlin, and J. Ross. Fast mixing of multi-scale langevin dynamics under the manifold hypothesis, 2020.
- R. Cai, G. Yang, H. Averbuch-Elor, Z. Hao, S. Belongie, N. Snavely, and B. Hariharan. Learning gradient fields for shape generation, 2020.
- N. Chen, Y. Zhang, H. Zen, R. J. Weiss, M. Norouzi, and W. Chan. Wavegrad: Estimating gradients for waveform generation, 2020.
- J. Chung, K. Kastner, L. Dinh, K. Goel, A. Courville, and Y. Bengio. A recurrent latent variable model for sequential data, 2015.
- S. Fogel, H. Averbuch-Elor, S. Cohen, S. Mazor, and R. Litman. Scrabblegan: Semi-supervised varying length handwritten text generation, 2020.
- I. Goodfellow, J. Pouget-Abadie, M. Mirza, B. Xu, D. Warde-Farley, S. Ozair, A. Courville, and Y. Bengio. Generative adversarial nets. In Z. Ghahramani, M. Welling, C. Cortes, N. D. Lawrence, and K. Q. Weinberger, editors, *Advances in Neural Information Processing Systems 27*, pages 2672–2680. Curran Associates, Inc., 2014. URL <http://papers.nips.cc/paper/5423-generative-adversarial-nets.pdf>.
- A. Graves. Generating sequences with recurrent neural networks, 2013.
- M. Heusel, H. Ramsauer, T. Unterthiner, B. Nessler, and S. Hochreiter. Gans trained by a two time-scale update rule converge to a local nash equilibrium. In I. Guyon, U. V. Luxburg, S. Bengio, H. Wallach, R. Fergus, S. Vishwanathan, and R. Garnett, editors, *Advances in Neural Information Processing Systems 30*, pages 6626–6637. Curran Associates, Inc., 2017. URL <http://papers.nips.cc/paper/7240-gans-trained-by-a-two-time-scale-update-rule-converge-to-a-local-nash-equilibrium.pdf>.
- J. Ho, A. Jain, and P. Abbeel. Denoising diffusion probabilistic models, 2020.
- A. Jolicoeur-Martineau, R. Piché-Taillefer, R. T. des Combes, and I. Mitliagkas. Adversarial score matching and improved sampling for image generation, 2020.
- L. Kang, P. Riba, Y. Wang, M. Rusiñol, A. Fornés, and M. Villegas. Ganwriting: Content-conditioned generation of styled handwritten word images, 2020.

- V. Khruikov and I. Oseledets. Geometry score: A method for comparing generative adversarial networks, 2018.
- D. P. Kingma and J. Ba. Adam: A method for stochastic optimization, 2017.
- D. P. Kingma and M. Welling. Auto-encoding variational bayes, 2014.
- Z. Kong, W. Ping, J. Huang, K. Zhao, and B. Catanzaro. Diffwave: A versatile diffusion model for audio synthesis, 2020.
- A. Kotani, S. Tellex, and J. Tompkin. Generating handwriting via decoupled style descriptors, 2020.
- Q. Liu, J. D. Lee, and M. I. Jordan. A kernelized stein discrepancy for goodness-of-fit tests and model evaluation, 2016.
- M. Liwicki and H. Bunke. Iam-ondb - an on-line english sentence database acquired from handwritten text on a whiteboard. *Eighth International Conference on Document Analysis and Recognition (ICDAR'05)*, pages 956–961 Vol. 2, 2005.
- M. Mayr, M. Stumpf, A. Nikolaou, M. Seuret, A. Maier, and V. Christlein. Spatio-temporal handwriting imitation, 2020.
- T. Pang, K. Xu, C. Li, Y. Song, S. Ermon, and J. Zhu. Efficient learning of generative models via finite-difference score matching, 2020.
- M. Sandler, A. Howard, M. Zhu, A. Zhmoginov, and L.-C. Chen. Mobilenetv2: Inverted residuals and linear bottlenecks. pages 4510–4520, 06 2018. doi: 10.1109/CVPR.2018.00474.
- J. Sohl-Dickstein, E. A. Weiss, N. Maheswaranathan, and S. Ganguli. Deep unsupervised learning using nonequilibrium thermodynamics, 2015.
- Y. Song and S. Ermon. Generative modeling by estimating gradients of the data distribution, 2019.
- Y. Song and S. Ermon. Improved techniques for training score-based generative models, 2020.
- C. Szegedy, V. Vanhoucke, S. Ioffe, J. Shlens, and Z. Wojna. Rethinking the inception architecture for computer vision. 06 2016. doi: 10.1109/CVPR.2016.308.
- A. Vaswani, N. Shazeer, N. Parmar, J. Uszkoreit, L. Jones, A. N. Gomez, L. Kaiser, and I. Polosukhin. Attention is all you need. In I. Guyon, U. V. Luxburg, S. Bengio, H. Wallach, R. Fergus, S. Vishwanathan, and R. Garnett, editors, *Advances in Neural Information Processing Systems 30*, pages 5998–6008. Curran Associates, Inc., 2017. URL <http://papers.nips.cc/paper/7181-attention-is-all-you-need.pdf>.
- P. Vincent. A connection between score matching and denoising autoencoders. *Neural Computation*, 23:1661–1674, 2011.

A Architecture Details

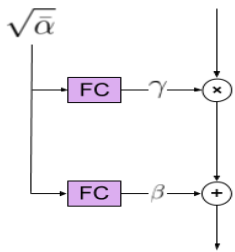


Figure 6: Our Conditional Affine Transformation.

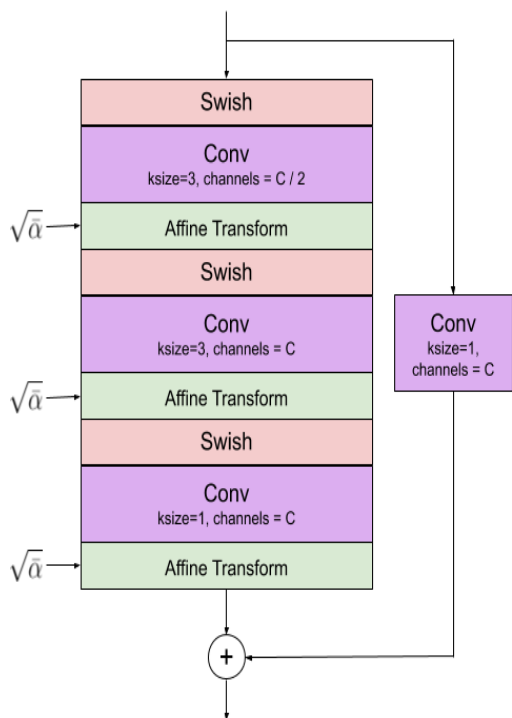


Figure 7: Our Convolutional block.

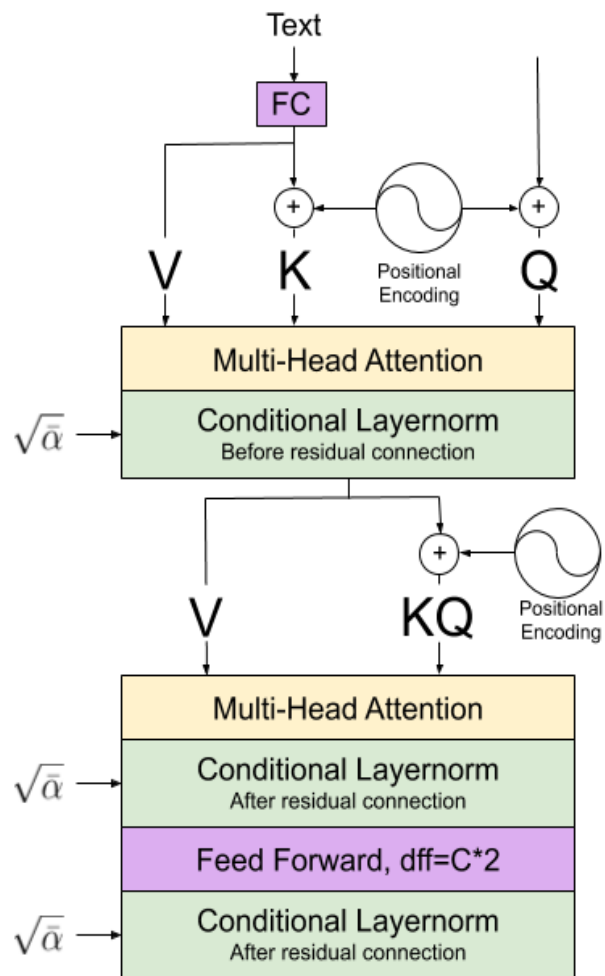


Figure 8: Our Attentional block.

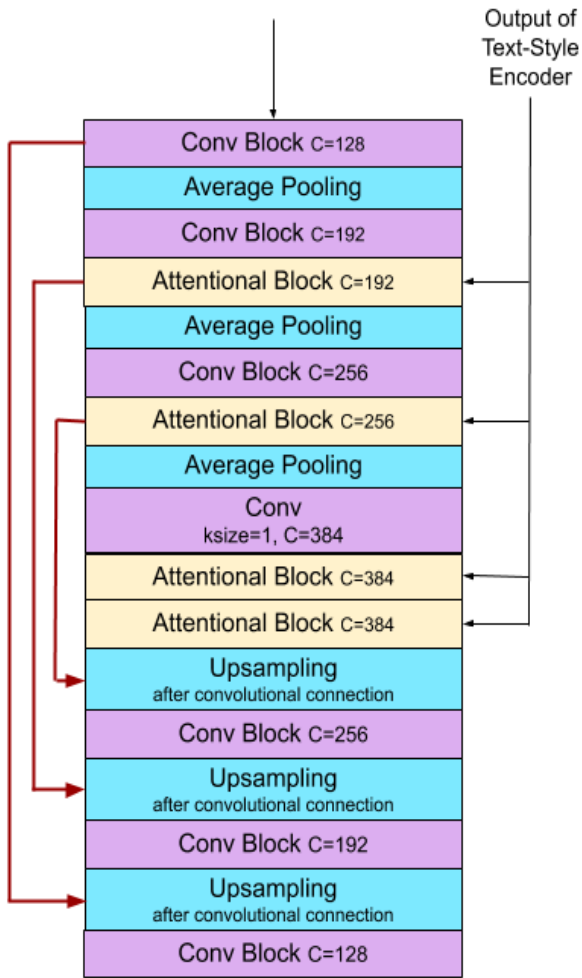


Figure 9: Architecture of the diffusion model.

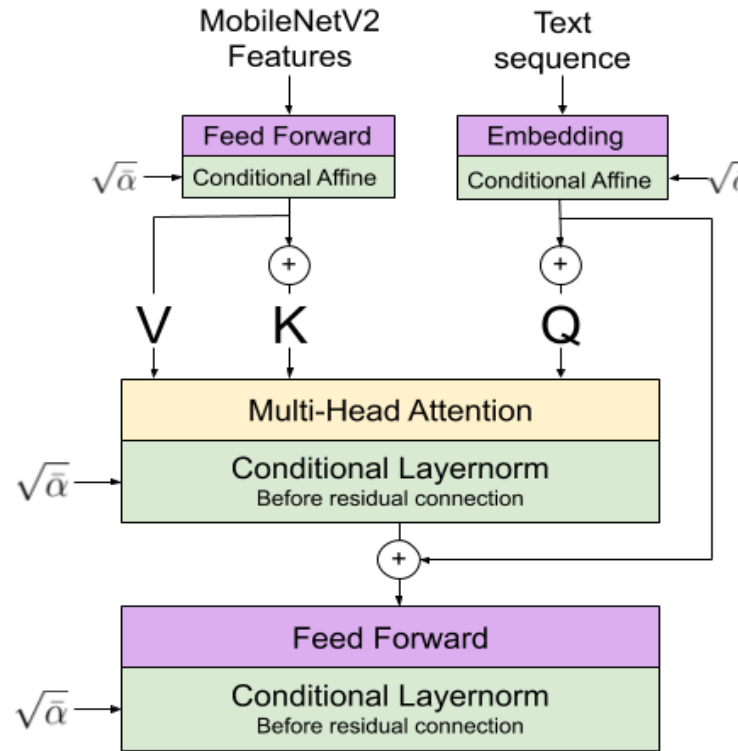


Figure 10: Architecture of the Encoder.

B Samples

The phrases "as I ever saw", "that the attractive forces", "the traverser had eaten", and "you will find a number of" in Figure 5 are real.

the quick brown fox jumps

the quick brown fox jumps

the quick brown fox jumps

the quick brown fox jumps

the quick brown fox jumps

the quick brown fox jumps

the quick brown fox jumps

the quick brown fox jumps

the quick brown fox jumps

Samples from a diffusion model

Samples from a diffusion model

Samples from a diffusion model

Samples from a diffusion model

Samples from a diffusion model

Samples from a diffusion model

Samples from a diffusion model

Samples from a diffusion model

Samples from a diffusion model

Figure 11: Samples generated from our model. On the left: "the quick brown fox jumps". On the right: "Samples from a diffusion model"

came through, tall and elegant

came through, tall and elegant

and he never seemed to get more

and he never seemed to get more

"I'd like to do that." Gavin

"I'd like to do that." Gavin

which brought .

which brought .

straight theodolite next. The

straight theodolite next. The

he remarked affably. "Do they?"

he remarked affably. "Do they?"

of war, when most lives were

of war, when most lives were

desperate need for funds.

desperate need for funds.

as I ever saw.

as I ever saw.

that the attractive forces

that the attractive forces

the matter remained thus, while

the matter remained thus, while

Seaver's Memory was prodigious.

Seaver's Memory was prodigious.

questions before us and

questions bore us and

probable that they would

probable that they would

not wholly closed to John

not wholly closed to John

that Magyar cookery owes

that Magyar cookery owes

Figure 12: Samples generated from our model.

lensky, Prime Minister
 lensky, Prime Minister
 had left it.
 had left it
 Fairbanks's conception. But
 Fairbanks's conception. But
 who suggested that this
 who suggested that this
 Gavin had gone outside when Larry
 Gavin had gone outside when Larry
 sweetest wife in the world
 sweetest wife in the world
 "It is a pity," said Mart,
 "It is a pity," said Mart,
 unforeseen forces of birth,
 unforeseen forces of birth,

pointing to murder .
 pointing to murder .
 engines and flung open the canopy.
 engines and flung open the canopy.
 that air of improvisation ,
 that air of improvisation ,
 Mrs. Lawford. There are a
 Mrs. Lawford. There are a
 consequently a folklore of song, festival
 consequently a folklore of song, festival
 South. This rapid movement in the
 South. This rapid movement in the
 SD was the standard deviation
 SD was the standard deviation
 In the first place, it has no clear
 In the first place, it has no clear

Figure 13: Samples generated from our model.

<p>night bring only a disturbed tossing night bring only a disturbed tossing night bring only a disturbed tossing night bring only a disturbed tossing night bring only a disturbed tossing night bring only a disturbed tossing night bring only a disturbed tossing night bring only a disturbed tossing</p>	<p>here in the same words in here in the same words in here in the same words in here in the same words in here in the same words in here in the same words in here in the same words in here in the same words in here in the same words in here in the same words in here in the same words in here in the same words in</p>
---	---

Figure 14: Samples generated from our model. Both of the texts, "night bring only a disturbed tossing" and "here in the same words in" are from the test dataset.

objectives.

It is most unfair to call "Plackias"

the samples appear to have been

the samples appear to have been

written by the same writer

written by the same writer

Figure 15: In each column, the top line is a sample of a writer from the test dataset's style. The bottom two lines are produced by the generative model using the style information s in the first line.

tatives of Sir Roy We-	tatives of Sir Roy We-
tatives of Sir Roy We-	tatives of Sir Roy We-
men he believes in his "destiny." His	men he believes in his "destiny." His
men he believes in his "destiny." His	men he believes in his "destiny." His
the car at the point	the car at the point
the car at the point	the car at the point
one of its most classic	one of its most classic
one of its most classic	one of its most classic
lodged upon his nose what he	lodged upon his nose what he
lodged upon his nose what he	lodged upon his nose what he
voice crackled over the wire.	voice crackled over the wire.
voice crackled over the wire.	voice crackled over the wire.
lecture is provided along with	lecture is provided along with
lecture is provided along with	lecture is provided along with
structure. The objectives.	structure. The objectives.
structure, the objectives.	structure. The objectives.

Figure 16: The left column shows samples from the *ablated* model, which uses Equation 9 to compute y_{t-1} . The right column shows samples from our final model.

across the grain, holding the plane

across the grain, holding the plane

didn't over-indulge.

didn't over-indulge.

with these. As an elementary

with these. As an elementary

stones."

stones."

Besides, if one looks at the

Besides, if one looks at the

to the other door. Everything

to the other door. Everything

that lay totally outside

that lay totally outside

and protons which comprise

and protons which comprise

across the grain, holding the plane

across the grain, holding the plane

didn't over-indulge.

didn't over-indulge.

with these. As an elementary

with these. As an elementary

stones."

stones."

Besides, if one looks at the

Besides, if one looks at the

to the other door. Everything

to the other door. Everything

that lay totally outside

that lay totally outside

and protons which comprise

and protons which comprise

Figure 17: The left column shows samples from the *ablated* model, which uses Equation 9 to compute y_{t-1} . The right column shows samples from our final model.